Inkjet Printing of Epidermal RFID Antennas by Self-Sintering Conductive Ink

S. Amendola, A. Palombi and G. Marrocco

***Abstract*—The recently introduced inkjet printing technology with ambient-sintering is here investigated for the fabrication of epidermal antennas suitable for Radiofrequency Identification (RFID) and Sensing. The attractive feature of this manufacturing process is the possibility to use low-cost printers without any high-temperature curing.**

In spite of the estimated maximum achievable conductivity of the ink ($\sigma_{UHF} = 1 \times 10^5$ S/m) in UHF-RFID band is two orders of magnitude lower than that of the bulk copper, a three-fold printing process provides the same on-skin radiating performance as manufacturing technologies using bulk conductors.

Experiments demonstrate that the epidermal antennas printed on PET substrate are insensitive to moderate mechanical stress, like the natural bending occurring over the human body, and to the possible exposure to body fluids (e.g. sweat). Moreover, the electromagnetic response remains stable over the time when the printed layouts are coated with biocompatible membranes.

***Index Terms*—Radiofrequency Identification, RFID tags, wearable sensor, wireless sensor, body sensor network, UHF antennas, ink-jet printing, additive manufacturing.**

I. Introduction

[1]Flexible and body-conformable sensors are a promising driver for the new generation of non-invasive and discrete body-centric systems with application to biomedicine, security and entertainment. The recent convergence between the emerging *Epidermal Electronics* [1] and the more assessed Radiofrequency Identification (RFID) technology for passive body-centric systems [2] is indeed stimulating the development of novel skin-tight battery-less devices provided with sensor capabilities and wireless interfaces for communication with a remote reader unit. Pioneering applications of epidermal RFID tags to the wireless measurement of body temperature and to wound healing monitoring were already demonstrated in [3], [4].

Reshaping RFID transponders, conventionally used in logistics of bulk objects, into a suitable layout for skin mounting, demands for techniques to deposit conductive traces over biocompatible ultra-thin flexible membranes. Cost-effective and easily accessible methods are hence required for both the rapid prototyping of laboratory samples as well as for the mass production of skin sensors over the large scale. The first referred prototypes of *tattoo*-like tags, in the UHF RFID band (860 - 960 MHz), were fabricated by profiling conductive silver painting or a nickel-based screening spray by means of the stencil technique [5].

[1]Paper submitted on August 6th 2016, revised on November 27th 2017, and resubmitted on July 6th 2017. The authors are with the Pervasive Elecromagnetics Lab, www.pervasive.ing.uniroma2.it, upon the University of Roma Tor Vergata, Italy. Reference: amendola@info.uniroma2.it

Inkjet printing is a promising technology for depositing metal traces on flexible and even stretchable substrates [6], [7], [8]. This process is being increasingly adopted by the electronics industry for the fabrication of RF circuits and wireless devices [9] by using electrically engineered inks made by metallic nanoparticle, conductive polymers (PEDOT-PSS), organometallic compounds and carbon nanotubes (refer to [10], [11] for a complete survey). Inkjet printing of silver nano-particle inks has been already experimented also for manufacturing RFID tags [12], [13] and even to produce epidermal antennas over transfer tattoo paper [14]. Most of the published works refers to highly specialized and expensive printing equipments, like the FUJIFILM Dimatix DMP-2800, with nanoparticle silver-based inks (e.g. from Xerox, Sigma Aldrich). This technology requires thermal or laser post-deposition sintering treatments at high temperature (between 135 and more than 300 degrees) to provoke the coalescence of the nanoparticles that are enclosed in a polymeric shell - specifically designed to forbid agglomeration prior to the deposition - and, accordingly, to achieve the optimal electrical conductivity.

Depending on the specific printing process, the kind of substrate, the number of the printed layers and the resulting thickness of the traces, the dc conductivity of printed ink nowadays approaches the same order of magnitude ($\sigma \div 10^7$ S/m) as bulk conductors ($\sigma(Ag) = 6.3 \times 10^7$ S/m, $\sigma(Cu) = 5.9 \times 10^7$ S/m, $\sigma(Al) = 3.5 \times 10^7$ S/m). Just to give an example, a conductivity of $\sigma = 2 \times 10^7$ S/m was measured at 2450 MHz in [15] for a silver-based ink printed on cardboard and thermally cured.

Very recent progresses in Materials Science originated a new class of conducting inks [16], [17] which dry at room temperature and form an instantly conductive layer, without the need of time-consuming thermal sintering [18], [19]. These sintering-free inks are hence suitable to be cheaply and easily deposited on a flexible substrate by using consumer-grade, low-cost, inkjet printers. The feasibility of the fabrication of a variety of functional electronic prototypes, including touch and proximity-sensitive surfaces and capacitive liquid-level sensors, have been already demonstrated in [20], [21]. The same authors proposed in [22] procedures to make interconnections between double sided patterns with the purpose of fabricating multilayered instant-printed circuits. Even more recently, the self-sintering ink was used for the fabrication of miniaturized artificial magnetic conductors in the sub-GHz applications [23] and for the manufacturing of chipless humidity RFID sensors [24]. The declared spatial resolution of the printed trace was

150 μm while the ink sheet resistance was estimated to be 0.3 Ω/m (with no indication about the number of printed layers).

The application of the above manufacturing technique to epidermal antennas working in the UHF-RFID band requires a more in-depth analysis to take care of a number of additional parameters which are specific to the co-habitation of an antenna with the human skin, such as the printing quality over common biocompatible substrates, the presence of the sweat, the possible bending over body curvatures and the need of a protective coating.

In spite of some information about the radiofrequency feature of the self-sintering inkjet printing of antennas may be derived from above cited papers, other issues such as the achievable conductivity versus the specific inkjet process (say the number of printed layers), the long-term performance, the robustness to the mechanical and chemical stress, are still unknown and worthwhile of further investigation.

Thus, this work describes a complete and independent characterization of the Self-Sintering ink-jet technology for the specific fabrication of epidermal antennas with the overall goal of identifying the most appropriate modalities to achieve read-range performance as close as possible to the bulk copper in case of application onto the skin, and to test the sensitivity of the ink-jet printed antennas in variable boundary conditions typical of body-centric systems. The basics of the sintering-free conductive ink are reviewed in Section II regarding the ink conductivity in the dc regime and the identification of suitable printing substrates. Then, the ink conductivity is estimated in the UHF-RFID band by means of a combined experimental/simulated identification procedure versus the number of printed layers (Section III). Section IV addresses the achievable performance of realistic epidermal antennas concerning the achievable realized gain versus the trace width, the resistance to bending and to body fluids and the stability over time. Some possible bio-compatible coatings are also experimented. Finally, the self-sintering printing technology is demonstrated for the real application over the skin and then compared (Section V) with other conventional manufacturing options involving bulk conductors that have been already proposed for epidermal antennas.

II. Self-Sintering Ag Ink

The silver nano ink from Mitsubishi Paper Mill [16] consists of an aqueous solution containing silver nanoparticles of approximately 20 nm diameter uniformly dispersed in a solvent consisting of polymer latex and a halide emulsion. The conductivity of this ink spontaneously emerges at ambient temperature as soon as the solution is dried, thanks to the formation of interconnections among the silver nanoparticles which is triggered by the halide [27]. The printer selected for the ink deposition was the Brother MFC-J5910DW whose specific nozzles eject higher volumes of ink than other printers, meaning that a greater amounts of conductive ink can be deposited in a short time. The standard CMYK cartridges were all refilled by the Ag-ink using disposable syringe filters. The print quality is 6000x1200 dpi. Accordingly, in comparison with a single-nozzle printer, the considered printing process releases four times the amount of ink that roughly correspond to four layers. However, unlike professional printers, this low-cost procedure does not permit any kind of control over the inkjet process like the size of the droplet, the temperature of the nozzle, the time between two consecutive droplets so that the appearance of the resulting trace could be different between the two procedures. To prevent confusion, the term "layer" is hereafter avoided while the term "single-printed trace" will refer to the output of the printer, as it is.

A. Suitable printing substrates

The first step of the research considered the possibility to deposit this ink over sheets and membranes suitable to host epidermal devices such as ink-jet tattoo-paper, polyurethane-based dressing, cellulose membrane, adhesive non-woven fabrics. Tattoo transfer paper, in particular, has been already experimented for printing silver ink dispersed in organic solvent and then sintered at 135 °C [14]. Two additional media suggested by the ink manufacturer were also considered: a resin-coated paper and a PET film (white or transparent) having a PVA-based ink receptive layer on top [28].

The tested materials with the corresponding optical micrographs of a 2x10 mm^2 printed trace are listed in Table I. None of the skin-like membranes revealed adequate for self-sintering ink, as the dc impedance measured between the two extremities of the trace was higher than 2 MΩ. The ink penetrated within the fibrous matrix (4, 5), spread over hydrophobic surface (2) or formed evident cracks (1), thus preventing the activation of chemical sintering and the creation of a continuous conductive path. A low resistance was achieved only with the commercial printing sheets (6, 7) thanks to their specific surface treatment based on a porous coating layer that facilitates the ink adhesion and the solvent absorption at the nano-scale and prevents smearing. Although being flexible, thin and bio-compatible, the texture of these sheets is not entirely suited to intimately adhere to the skin; they have been used anyway in this study for the ink characterization for epidermal-oriented applications, while major efforts are being currently devoted to process the surface of the other more skin-like membranes to make them printable.

B. The spontaneous-sintering effect

Fig. 1(a) shows an example of the sheet resistance of a single-printed rectangular trace over PET substrate with size ratio Width/Length=100, according to the standard in [29]. The spontaneous chemical sintering of the ink activates right after the printing and it continues for the next 30 minutes with a progressive reduction (up to 17%) of the sheet resistance (R_S) down to its asymptotic value that is hereafter considered as the ink resistivity.

The resulting value of R_S is rather unaffected by the temperature of the printing environment, while it slightly reduces in case of high humidity conditions (Fig. 1(b)). The thickness of the profiles of printed traces, as measured by Dektak 3ST surface profilometer, is rather non-uniform with

Table I
FLEXIBLE SUBSTRATES TESTED FOR THE DEPOSITION OF SELF-SINTERING INK BY DESKTOP PRINTER.

Substrate	Optical micrograph (60x)
1.Ink-jet tattoo-paper Crafty computer paper 20 μm	
2. Polyurethane-based dressing Rollflex Master-Aid 22 μm	
3. Cellulose Membrane Visking Dialysis Medicell International ltd 30 μm	
4. Adhesive non-woven fabric Fixomull® Stretch 120 μm	
5. Adhesive non-woven fabric Amuchina 70 μm	
6. Resin coated paper Mitsubishi Paper Mills 177 μm	
7. PVA coated PET Mitsubishi Paper Mills 135 μm	

an average value $t = 470$ nm due to ink agglomeration and substrate porosity (Fig. 2).

The overall average sheet resistance derived from multiple measurements is $R_S = 0.22$ Ω/sq and the corresponding conductivity in dc can be hence estimated as:

$$\sigma_{DC} = \frac{1}{R_S t} \approx 1 \cdot 10^7 S/m \tag{1}$$

which is just a quarter of that of bulk conductor and also in line with the values reported in literature for the artificial sintering-based conducting inks.

As it will be shown in the next Section, the conductivity in the UHF band is expected to be rather different due to the frequency dependance of the response of the non-metallic matters inside the composite ink.

III. INK CONDUCTIVITY IN THE UHF-RFID BAND VERSUS THE PRINTING PASSES

The conductivity of printed traces, as for more conventional conducting ink, is dependent on the number of printed layers.

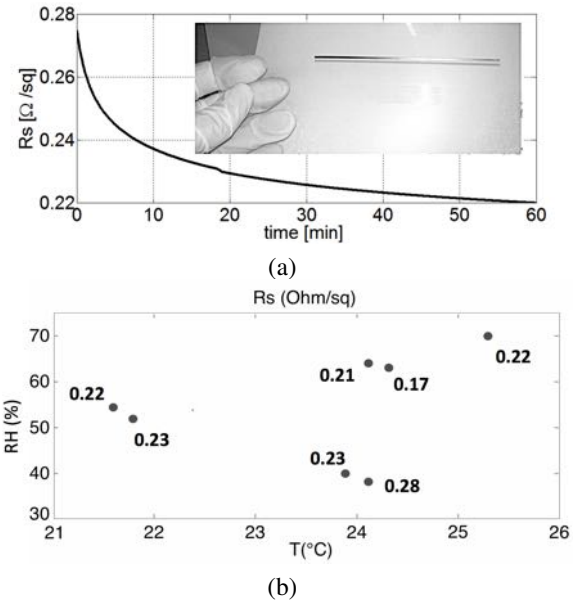

Figure 1. a) Time-variant dc sheet resistance (in Ω/sq) of a printed *W/L*=100 trace on PET transparent film as measured at ambient conditions (*T* = 24.1°C and relative humidity *RH* = 64%). Time *t*=0 marks the end of the print procedure. b) Sheet resistance of several printed traces on PET for variable ambient conditions during the printing process.

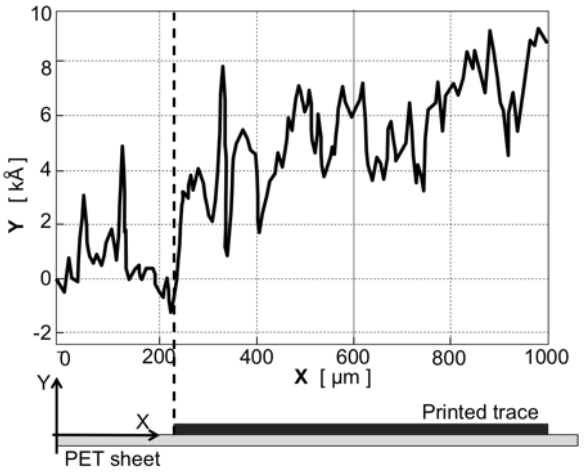

Figure 2. Measured profile (by Dektak 3ST surface profilometer) of the inkjet printed trace on PVA-coated PET film.

The considered desktop printer does not permit to freely control the amount of deposition, thus the only way to test the overprinting effect is re-loading several times the same sheet for a new printing task at the purpose to increase the ink density.

Common techniques to estimate the surface impedance at microwave frequencies are usually based on the measurement of the insertion loss of microstrip lines [15] as well as on the estimation of the quality factor in narrowband resonant cavities [30] or on wideband transmission/reflection measurements in

guided devices ([31]). In this work the RF conductivity of the Ag-ink in the UHF band versus the number of print layers was instead derived by an alternative method involving a single port measurement of a resonant antenna and a parameter-identification procedure. For this purpose, a numerical model of the antenna needs to be matched, with respect to the unknown conductivity of its traces, to the measured reflection coefficient (S_{11}) of the corresponding prototype. A similar method was already applied for the characterization of conducting polymers loading an RFID antenna in [32].

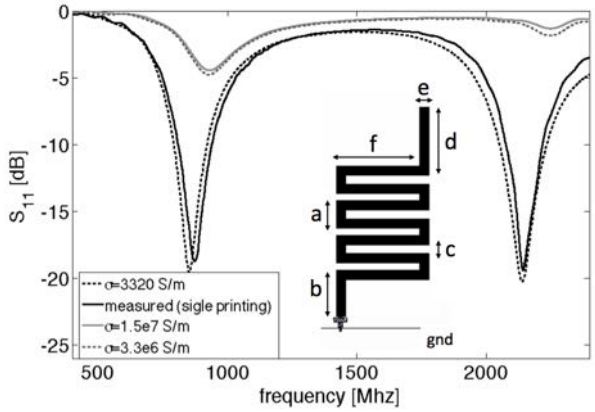

Figure 3. Meandered monopole used as reference antenna for the identification of the ink conductivity. Size [mm]: *a*=5.7, *b*=10, *c*=1.7, *d*=14, *e*=2, f=17. Comparison between the measured S_{11} of the printed MLA and the simulated response of the corresponding FDTD model including the identified conductivity in the UHF band. The response obtained with the dc conductivity (1.5×10^6 S/m) and the RF conductivity (3.3×10^6 S/m) deduced by [24] is also reported for comparison.

The considered test antenna was a meander-line monopole (MLA, inset of Fig. 3) to take benefit from the presence of the transmission line current mode in the meanders generated by the multiple foldings [33], [34] that induces a huge sensitivity of the antenna response to the conductivity of the traces. The monopole was designed to have the first two series resonances around 900 MHz and 2450 MHz, respectively.

The printed monopole was placed over a copper ground plane and connected to a SMA connector via a two-parts conductive epoxy glue (CircuitWorks®CW2400 by Chemtronics, 20 min curing at 55°C). The dielectric properties of the printing substrate ($\varepsilon = 1.9$, $\sigma = 0.015$ S/m) were previously derived through the method described in [37]. The reflection coefficient S_{11} was hence measured in the frequency band 300-3000 MHz through a Vector Network Analyzer. Then, the same layout was modeled by Finite-Difference Time-Domain (FDTD) method (CST Microwave Studio 2016) and the following penalty function was minimized to identify the unknown trace effective conductivity:

$$s = \sum_{n=1}^{2} \begin{array}{l} w_1|f_{n,meas} - f_{n,sim}(\sigma)|+ \\ +w_2|B_{meas}(f_n) - B_{n,sim}(f_n,\sigma)|+ \\ +w_3|S_{11,meas}(f_n) - S_{11,sim}(f_n,\sigma) - 5| \end{array} \quad (2)$$

where $\{f_1,f_2\}$ are the first two resonant frequencies of the MLA around the UHF band, $S_{11}(f_n)$ the reflection coefficient at these resonances (expressed in dB), $B(f_n)$ the bandwidth referred to $S_{11} = -10\,dB$ around the resonances and $w_1 = w_2 = 0.2$, $w_3 = 0.1$ the weighing coefficients. Minimization was achieved by using the *Trust Region Framework* method by varying the conductivity of the numerical model.

Fig. 3 shows the measured S_{11} (averaged over five printed prototypes made by a single-pass printing) which exhibits two sharp nulls around 870 MHz and 2100 MHz. The identified effective RF conductivity was $\sigma_{UHF}(pass = 1) = 3.3{\cdot}10^3$ S/m and hence sensibly lower (four orders of magnitude) than the corresponding dc value. Indeed, unlike pure metals, the self-sintering ink is characterized by a considerable frequency-dependent behavior due to the composite nature of the ink (conductive filler within a polymer matrix) and the residual presence of non-conductive materials (binders, solvents and additives) after the spontaneous sintering which introduce extra losses [8].

The measurements were then repeated for an increasing number of printing passes. The microstructure of the pattern evolves, as illustrated by the Surface SEM photographs (magnification of 100Kx) in Fig. 4(a). A significant densification and coarsening of the silver grains is produced by the spontaneous coalescence of metallic nanoparticles when increasing the number of the printing layers from one to four.

A lower magnification image (500x, Fig. 4(b)) shows that the use of a low-cost desktop inkjet printer led to an irregular profile of the edge of the printed trace, with ink dots spread around the edge. Moreover, the tray-based paper loading mechanism produces unavoidable overall misalignments of up to 0.2-0.5 mm when the substrate is manually re-inserted into the printer distributor for additional ink release. Overall, the resulting effect is the widening and blurring of the trace with a local reduction of the effective conductivity close to the edge of the trace. Thus, to profitably apply this overprinting procedure, the antenna shouldn't have traces thinner than 1 mm.

The conductivity achieved in the case of *n*={1, 2, 3, 4} printing passes was estimated through the above identification procedure and listed in Tab. II. The resulting values increases by up to two orders of magnitude ($\sigma \approx 10^5$) when overprinting the antenna three times (*n*=4 passes). It is worth noticing that the retrieved conductivities are substantially lower than the value $\sigma_{ref} = 3.3 \cdot 10^6$ S/m that can be deduced from [23] by applying eq. (1) for the declared parameters R_S=0.3 Ω/sq and *t*=1μm. However, by introducing the latter value in the numerical modeling of the MLA, the corresponding S_{11} profile is rather divergent from the measured data (again in Fig. 3). This fact, and the further comparison between modeling and measurement of epidermal antennas shown in the next Section IV, seem to corroborate the lower value of conductivity as found here. The mismatch with [23] could be probably due to the manufacturing batch of the ink, as well as to different state of preservation before printing (transportation chain) and/or inside the printing cartridges themselves.

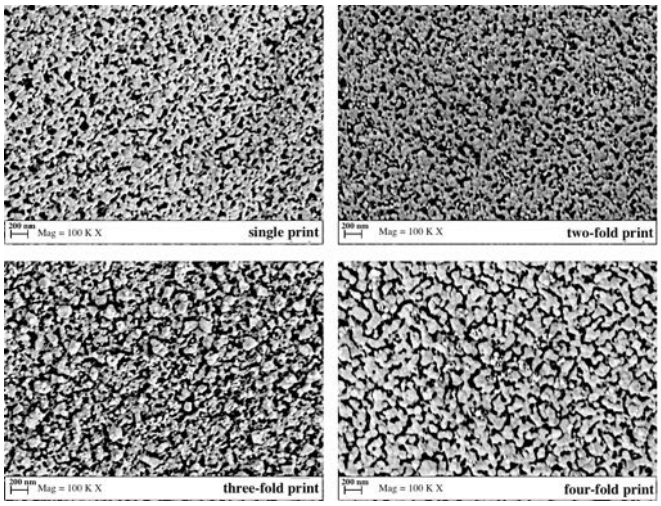

a)

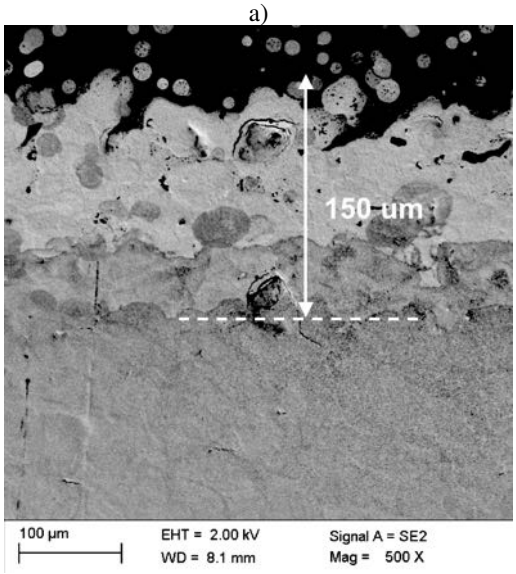

b)

Figure 4. SEM micrographs a) (100Kx) showing the macrostructural evolution of the granular conductive patterns as a function of the number of printing passes. b) 500x magnification of the trace edge in case of four-pass printing

IV. Application to Epidermal RFID antennas

The applicability of the considered inkjet printed technology to epidermal RFID sensor tags is now discussed by the help of an example of a meandered rectangular loop (2.5×5 cm^2) radiating like a two-C dipoles [3]. The radiator was connected to the EM4325 RFID microchip, which embeds an internal temperature sensor, by means of a T-match transformer properly shaped to achieve impedance matching (Z_{in}=23-j145 Ω at 870 MHz). The geometrical parameters of the antenna were optimized by means of numerical simulations accounting for the estimated conductivity of inkjet-printed traces for the application over a plastic box (PET ε_r= 2, $tan\delta$ = 0.005 @1GHz) filled with a liquid mixture (HSL900V2 by Speag®, $\epsilon_r = 41.2$, σ=0.95 S/m) mimicking the electromagnetic properties of

Table II
Estimated UHF conductivity vs. number of printings

Printing configurations	σ (S/m)
single print	$3.3e3$
two-fold print	$2.2e4$
three-fold print	$6.3e4$
four-fold print	$1e5$

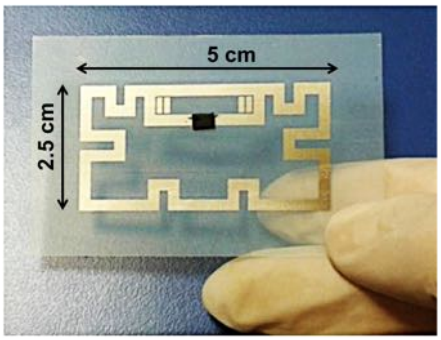

(a)

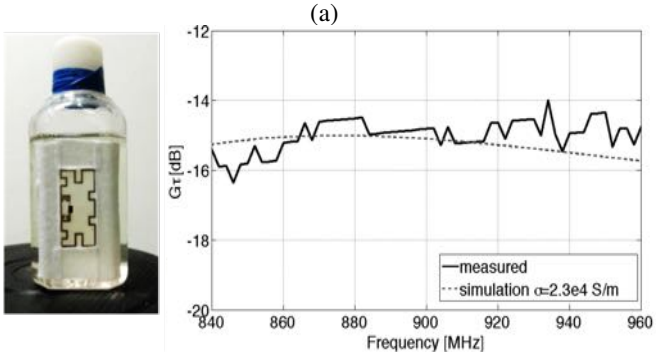

(b)

Figure 5. a) Inkjet-printed meandered-loop epidermal antenna over PET substrate. b) Simulated and measured realized gain (broadside direction) when the tag is attached onto a liquid phantom simulating the human body.

human tissues. The printed antenna was connected to the IC through the silver-based conductive glue. The resulting RFID tag was experimentally characterized in terms of the realized gain - defined as the power gain of the tag (along the broadside direction) multiplied by the power transfer coefficient between the antenna and the chip - which is directly related to the read range of the sensor. This performance indicator was measured by the turn-on power method, i.e. the tag was interrogated by an RFID reader at fixed distance (25 cm) with increasing power until the tag starts responding.

The comparison in Fig.5 between simulated and measured realized gain shows a good agreement in the world-wide RFID band with a local error of less than $\pm$1dB, thus corroborating the correctness of the estimated conductivity in the UHF band.

Fig. 6 shows the measured realized gain when the tag was fabricated by multiple overprinting as described above. The experimental outcomes are in full agreement with the numer-

ical model. The realized gain increases by about 1 dB per overprint so that nearly bulk copper performance is achieved with just three-fold printings and no practical advantage has to be expected with further release of the conducting ink. Since the reading range is related to the square root of the tag's realized gain, the expected benefit of the threefold printing process w.r.t. the single-printed antenna is a 25% increase in the range of the antenna.

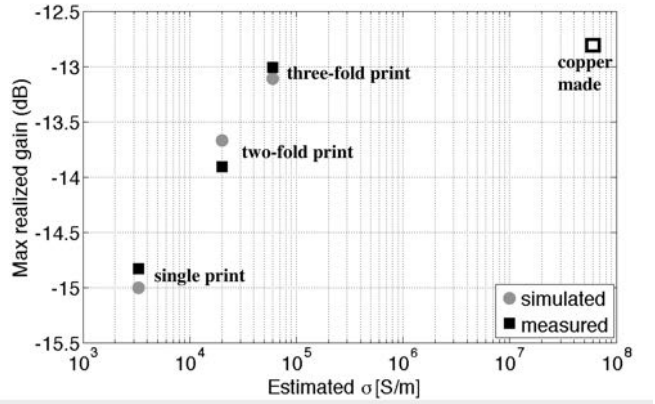

Figure 6. Maximum realized gain (measurements and simulations) of epidermal tag at 900 MHz as function of the estimated ink conductivity.

A. RF Performance versus the trace width

In order to derive the best compromise between the radiation performance (realized gain) of the inkjet printed epidermal antennas and the fabrication cost (i.e. the amount of used ink), the same layout as above was manufactured with traces having a smaller width $w = \{1,\ 0.5,\ 0.25\}$ mm. Case by case, the T-match section was slightly readapted to account for the corresponding impedance changes (mostly the imaginary part). To avoid the blurring effect due to multi-fold printing, and hence to drop out potential additional sources of uncertainty, only the case of single-pass ink release was considered.

Despite similar performance are expected from simulations regardless of the width of the antenna's traces, the measurements returned instead a rather different behavior. The comparison in Fig. 7(a) shows that the peak of realized gain slightly decreases (1 dB) when the trace is halved down to 1 mm but it is reduced by 5 dB in the case of 0.5 mm width. For thinner 0.25 mm traces the communication performance is further degraded down to the point where the tag was not readable at all from distance higher than 10 cm. Similar results were found in [35] concerning the sheet resistance measured in dc. As visible in the magnified detail of the 0.25 mm trace (Fig. 7(b)) several tiny perforations appear within the traces. As a consequence, when the width is less than 1 mm, there are not enough connected conductive clusters for electric current to flow. The degradation of the radiation performance of the narrower trace tags and the discrepancy with simulation is due to the fact that the estimated conductivity is an "effective" value that accounts for the non-uniform distribution of the silver nano-particles in the trace, and hence of the presence of discontinuous (low density) zones (holes). When the trace becomes narrower, the absolute reduction of the contiguous (interconnected) conductive path will strongly degrade the overall effective conductivity of the ink, while the simulation always uses a same constant value. Accordingly, for the considered printing procedure and materials, the 1 mm trace width could be considered as a practical and conservative lower bound.

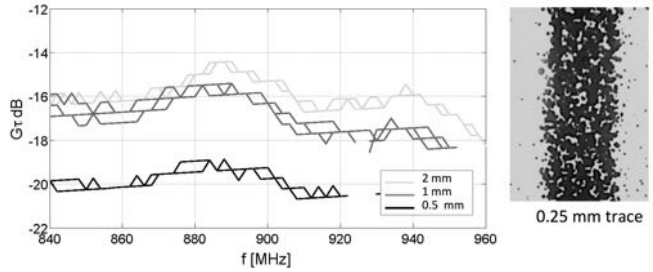

(a) (b)

Figure 7. (a) Measured realized gain of three couplets of epidermal antennas made by different trace width $w = \{2, 1,\ 0.5,\ 0.25\}mm$. (b) Magnified details (60x) of the 0.25 mm highly porous single-printed trace.

B. Resistance to bending and body fluids

Depending on the region of the body where the epidermal tag is attached on, it can be subjected to mechanical stresses due to the flexure over different body curvatures and to the repetitive bending around joints. Moreover, ink-jet printed layouts conceived for epidermal sensing applications can be exposed to moisture, including perspiration and sweat, especially in the case of printed resistive electrodes which cannot be insulated. It is hence crucial to assess the robustness of the considered ink against bending and exposure to body fluids which can both potentially affect the performance of the printed layout.

A threefold printed tag was hence subjected to a bending fatigue test by using the set-up described in [36], which consists of a stepper motor driving the central pin of a hinge with 12 mm radius (worst case, small curvature like a finger) (Fig. 8). The bending angle was swept from 0° to 180° for up to 2000 cycles at the speed of 12 cycles per minutes. Visual inspection by SEM microscope did not reveal any substantial change (micro-cracks/wrinkles/ or permanent folds) in the trace morphology before and after the fatigue test and the measured realized gain was invariant (See Fig. 9).

To assess the robustness of the ink against the exposure to the body fluids, the printed sample was initially placed inside a box at saturated vapor of a physiological solution (NaCl 9 gr/l) and then even immersed in the saline solution for several hours. In all the cases, the radiating performance of the tag measured after quick drying remained practically unchanged (Fig.9).

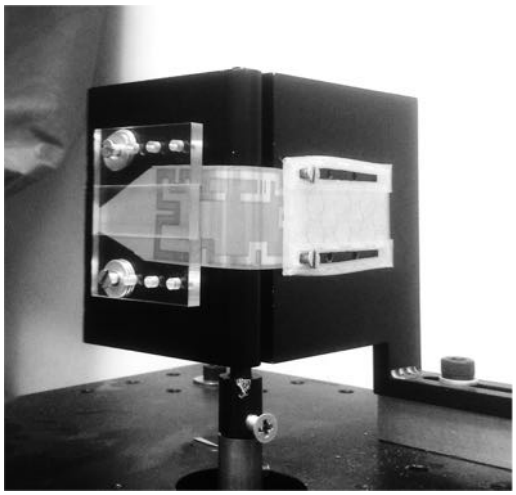

Figure 8. Ink-jet printed antenna mounted over a hinge set-up for the bending fatigue test.

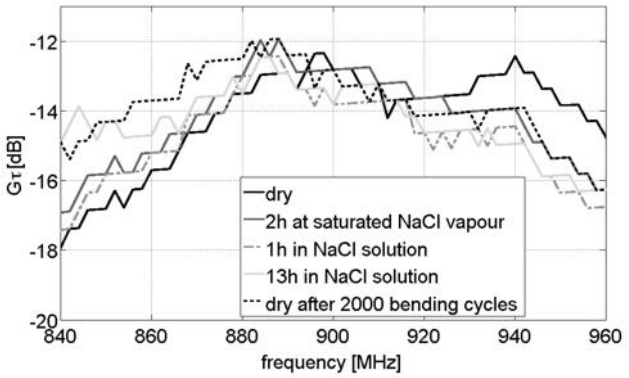

Figure 9. Measured realized gains of a threefold printed epidermal antenna before and after exposure to 100% RH, after immersion in saline solution and after 2000 of bending cycles.

C. Tag coating (Stability over time)

The conductivity of silver ink-jet printed layouts tends to degrade along with time in ambient air due to oxidation. A bio-compatible coating layer is hence required for the encapsulation of the antenna. Two possible encapsulations were considered: *1)* a silicon-based organic polymer (Polydimethylsiloxane PDMS) *2)* a medical-grade polyurethane ultra-thin (25μm) dressing (Rollflex from Master-AID).

The PDMS was prepared by mixing two liquid components (pre-polymer and cross-linking agent, Sylgard 184 by Dow Corning) - in a 10:1 mass ratio. The resulting viscous liquid was manually brushed over the printed traces and then cured at 60°C for 20 mins. The second film was instead directly stuck over the tag thanks to its adhesive backing.

The response along with time of bare and coated tags is compared in Fig.10. All the prototypes were printed simultaneously, i.e. at the same ambient conditions. The peak gain of the uncoated single-printed trace severely decreased (-4 dB)

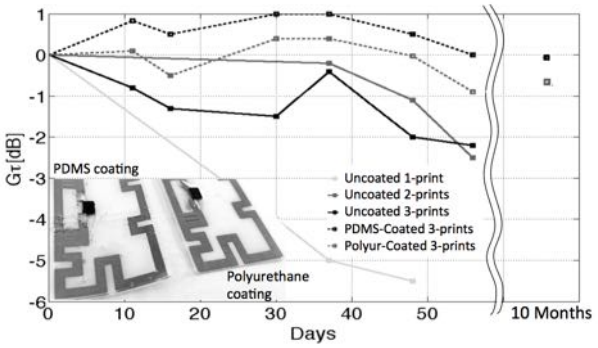

Figure 10. Variation of the maximum realized gain v.s. time of bare tags (single and overprinted) and coated tags with the respect of the initial value (printing time, t=0).

after one month, until becoming unreadable two weeks later. Overprinting process slows down the degradation ($\Delta G\tau$ =-2 dB after two months) as the oxidation process initially involves the most superficial ink layers. Both the polymeric coatings revealed adequate to protect the ink ensuring reasonably unaltered tags' gain, even 10 months after the fabrication.

It is worth noticing that the presence of the protective layer is not expected to affect the measurement of skin parameters as the possible sensitive parts of the tag could be left locally uncoated to permit the direct interaction with the underlying body tissues, while it has been previously verified in [3] that a thin layer does not alter the measurement of the skin temperature.

V. On-skin performance and comparison with conventional manufacturing techniques

The performance of the mono and threefold inkjet printed epidermal tags were finally evaluated in real on-skin placement and then compared with the response of the same layout fabricated with more conventional and assessed additive and subtractive manufacturing technologies involving bulk conductors (Fig. 11(a)):

i) flexible adhesive-backed copper foil (thickness 35 μm) carved by a two-axis digital-controlled cutting plotter;

ii) 120 μm-radius copper wire manually shaped, with the help of nails, over a double-sided adhesive tape;

iii) gold layer patterned over a ultra-thin (5-7 μm) polyimide substrate by means of flexible photolithography.

The last two solutions permit to achieve very thin and flexible antennas at the price of an expensive fabrication process (photolithography) and severe limitations in the geometry (microwire). The carved copper prototype looks instead bulky and less suitable to on-skin comfortable placements.

Each antenna was placed over the arm of a volunteer, at different times, by means of a 600 μm thick bio-silicone substrate (ε = 2.5, σ=0.005 S/m) and then fixed through an extremely thin (25 μm)) double-sided medical tape (3M™ 1509) (Fig. 11(b) and (c)). The bio-silicone layer was used as a separating membrane that partially confines the electric near-field of the antenna within the low-loss region of the substrate,

thus significantly reducing the power loss and improving the radiating performance, as extensively demonstrated in [38].

The corresponding measured realized gains are shown in Fig. 12. In spite of small mutual frequency shifts due to slightly different input impedance of the tags (indeed no post-manufacturing retuning was performed [3]), all the prototypes exhibited similar performance, with the peak value of the realized gain comprised between -15 dB and -11.5 dB and a rather broadband behavior. As expected from the previous investigations over phantoms, the mono-printed antenna returned a gain degradation of about 2-3 dB with respect to the bulk conductor prototypes while instead nearly identical performance was obtained by the threefold printed tag. Accordingly, the maximum achievable reading distance varies with the manufacturing process from 50 cm to 70 cm, when considering very low chip sensitivity for temperature sensing (P_{chip}=-4.5 dBm), and from 3.7 m to 5.2 m when considering *state-of-the-art* chip for labeling (P_{chip}=-22 dBm).

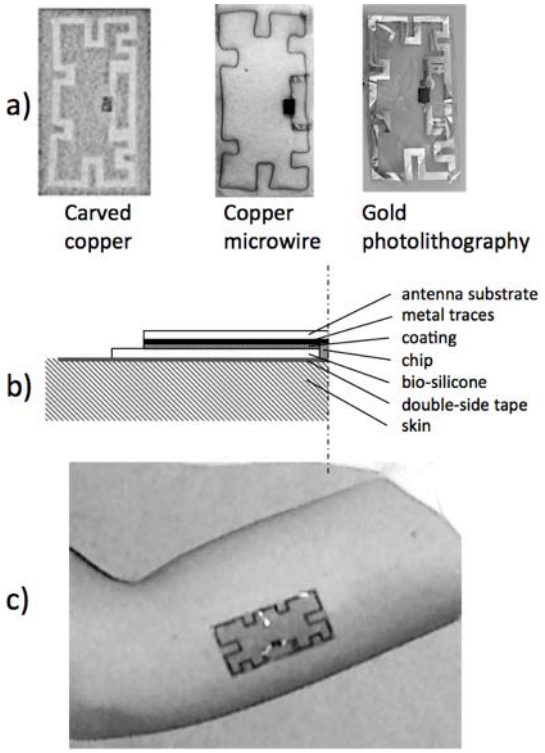

Figure 11. a) Prototypes of the test antenna made for comparison by three different manufacturing technologies; b) (half) cross-section of the corresponding integrated plasters. Depending on the antenna technologies, the *antenna substrate* is PET (inkjet), polyimide (photolithography) or biosilicone (copper-based methods) c) example of the placement over a volunteer's arm.

VI. Conclusions

The presented experimentations demonstrated that self-sintering conductive inkjet manufacturing with low-cost printers is a feasible technology for the fabrication of planar antennas suitable to epidermal radiofrequency identification and sensing.

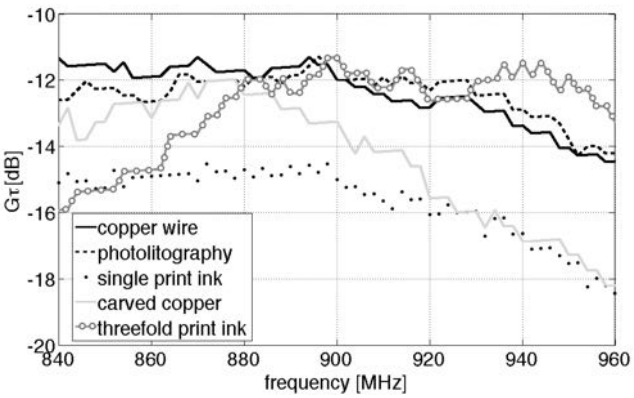

Figure 12. Measured Realized gains (broadside direction) vs. frequency of the epidermal tags attached over a volunteer's arm as in Fig. 11.

In spite of the few degrees of freedom in controlling the manufacturing process, self-sintering ink-jet printing can be easily tuned to achieve epidermal antennas with the same radiation performance of the bulk copper provided that three-fold printing is performed. Nevertheless, suboptimal printing could still be attractive for a very quick and low-cost intermediate prototyping and tests when a modest reduction of the read distance could be tolerated.

The printed traces are resistant against repeated cycles of bending, and hence the antenna could be suitable to comply with the natural deformation of the human body. The printing resolution is mostly imposed by the quality of the printer nozzle. By accounting also for the effective conductivity of mono-print layouts and for misplacements occurring during the overprinting, the minimum practical size of a trace should be roughly 1 mm. This looks enough for conventional UHF meandered dipole and loop antennas and for the interconnection to strap and TSSOP chip packages. This lower bound could be however inadequate for the fabrication of fine detailed patterns like multi-turn coils and the interconnecting lines of a QFN chip package, as also discussed in [26].

Concerning the printing substrate, PET film is an excellent biocompatible medium to produce robust printed prototypes of epidermal antennas. Nevertheless, additional research is needed to find self-sintering ink-compatible elastic and stretchable membranes that are really suitable to a comfortable application over the human skin. On the basis of recently published papers [39], a promising solution could be the use of biocompatible and biodegradable substrates based on poly(caprolactone) (PCL) and poly(lactic acid) (PLA), either in form of dense film and non-woven fibrous fabrics that might undergo suitable surface treatments. The resulting membranes are expected to have mechanical properties comparable to skin dermis along with a bunch of many other interesting properties such as drug releasing and cell culturing platform.

References

[1] J. Rogers, R. Ghaffari, D.H. Kim, *Strechable Bioelectronics for Medical Devices and Systems*, Springer, 2016

[2] S. Manzari, C. Occhiuzzi, G. Marrocco, "Feasibility of Body-Centric Systems Using Passive Textile RFID Tags", *IEEE Antennas Propagat. Magaz*., Vol.54 N.4 pp.49-62, Aug. 2012

[3] S. Amendola, G. Bovesecchi, A. Palombi, P. Coppa and G. Marrocco, "Design, Calibration and Experimentation of an Epidermal RFID sensor for remote Temperature Monitoring", *Sensors Journal, IEEE,* July 2016.

[4] C.Occhiuzzi, A. Ajovalasitb, M.A. Sabatino, C. Dispenza., G. Marrocco, M. Leone, "RFID Epidermal Sensor including Hydrogel Membranes for Wound Monitoring and Healing", submitted to 9^{th} *Annual IEEE International Conference on RFID*, San Diego, CA, April 2015.

[5] M. A. Ziai, J. C. Batchelor, "Temporary On-Skin Passive UHF RFID Transfer Tag", *IEEE Trans. Antennas Propagat.*, Vol.59, N.10, pp.3565-3571, Oct. 2011.

[6] Yin, ZhouPing, et al. "Inkjet printing for flexible electronics: Materials, processes and equipments.", Chinese Science Bulletin, Vol. 55, no.30, pp. 3383-3407, Oct. 2010.

[7] S. Khan, L. Lorenzelli, R.S. Dahiya, "Technologies for Printing Sensors and Electronics Over Large Flexible Substrates: A Review," in *Sensors Journal, IEEE ,* vol.15, no.6, pp.3164-3185, June 2015.

[8] Merilampi, Sari, T. Laine-Ma, and Pekka Ruuskanen. "The characterization of electrically conductive silver ink patterns on flexible substrates." *Microelectronics reliability*, Vol. 49, no. 7, pp. 782-790, July 2009.

[9] Cook, Benjamin S., et al. "Only skin deep: Inkjet-printed zero-power sensors for large-scale RFID-integrated smart skins.", *IEEE Microwave Magazine*, Vol. 14, no.3, pp. 103-114, 2013.

[10] M. Singh, H. M. Haverinen, P. Dhagat, G. E. Jabbour, "Inkjet Printing - Process and its Applications", *Advanced Materials*, Vol.22, pp. 673 - 685, 2010

[11] G. Cummins, M. P.Y. Desmulliez, "Inkjet printing of conductive materials: a review", *Circuit World*, Vol.38, N.4, pp.193-2013, 2012

[12] J. Side´n, M.K. Fein, A. Koptyug, H.-E. Nilsson, "Printed antennas with variable conductive ink layer thickness", *IET Microw. Antennas Propag*., Vol, 1, N.2 , pp. 401–407, 2007

[13] K. Koski, E. Koski, J. Virtanen, T. Bjorninen, L. Sydanheimo, L. Ukkonen, A. Z. Elsherbeni, "Inkjet-printed passive UHF RFID tags: review and performance evaluation", *Int. J. Adv. Manuf. Tecnol.* Vol.62 pp. 167-182, 2012

[14] V. Sanchez-Romaguera et al., "Towards inkjet-printed low cost passive UHF RFID skin mounted tattoo paper tags based on silver nanoparticle inks", *J. Mater. Chem. C*, pp. 6395-6402, 2013.

[15] H. Saghlatoon, L. Sydanheimo, L. Ukkonen, M. Tentzeris, "Optimization of Inkjet Printing of Patch Antennas on Low-Cost Fibrous Substrates", *IEEE Antennas and Wireless Propagation Letters*, Vol. 12, pp. 915-918, 2014

[16] NBSIJ Diamond Jet Silver Nanoparticle Ink, Mitsubishi Imaging (MPM), Inc., Available online at http://diamond-jet.com/silvernanoparticleink-2.aspx.

[17] Conductive Inkjet Ink 9101, Methode Electronics, Inc., Available online at http://www.methode.com/Documents/TechnicalLibrary/MDC_Inks_Conductive_Inkjet_Ink_9101_Data_Sheet.pdf.

[18] S. Magdassi, et al. "Triggering the sintering of silver nanoparticles at room temperature", *ACS nano*, vol.4, no.4, pp. 1943-1948, 2010.

[19] M. Grouchko, et al. "Conductive inks with a "built-in" mechanism that enables sintering at room temperature", *ACS nano,* vol.5 no.4 , pp. 3354-3359, 2011.

[20] Y. Kawahara, S.Hogdes, B. S. Cook, C. Zhang, G. D. Abowd, "Instant Inkjet Circuits: Lab-based Inkjet Printing to Support Rapid Prototyping of UbiComp Devices", *Proceedings of the 2013 ACM international joint conference on Pervasive and ubiquitous computing, ACM, 2013,* pp. 363-372.

[21] Y. Kawahara, S. Hodges, N. W. Gong, S. Olberding and J. Steimle, "Building Functional Prototypes Using Conductive Inkjet Printing," in I*EEE Pervasive Computing*, vol. 13, no. 3, pp. 30-38, July-Sept. 2014.

[22] Ta, Tung, et al., "Interconnection and double layer for flexible electronic circuit with instant inkjet circuits." *Proceedings of the 2015 ACM International Joint Conference on Pervasive and Ubiquitous Computing. ACM, 2015,* pp. 181-190.

[23] S. Genovesi, F. Costa, F. Fanciulli, A. Monorchio, "Wearable Inkjet-Printed Wideband Antenna by Using Miniaturized AMC for Sub-GHz Applications", *IEEE Antennas and Wireless. Propagat. Lett.*, Vol.14, pp. 1927-1930, 2016.

[24] M. Borghese, F.A. Dicandia, F. Costa, S. Genovesi, G. Manara, "An Inkjet Printed Chipless RFID Sensor for Wireless Humidity Monitoring", *IEEE Sensor Journal*, 2017 in Press

[25] Mansour, A. M., *et al.* "Efficient Design of Flexible and Low Cost Paper-Based Inkjet-Printed Antenna", *International Journal of Antennas and Propagation*, 2015.

[26] King, Philip H., J.Scanlan, A. Sóbester. "From Radiosonde to Papersonde: The Use of Conductive Inkjet Printing in the Massive Atmospheric Volume Instrumentation System (MAVIS) Project.", AIAA Infotech@ Aerospace. 2015. 0985.

[27] T. Yoshiki, S. Shino, K. Kobayashi, K. *Process for preparing conductive material*, United States Patent, US 8012676 B2, 2011.

[28] NB-TP-3GU100 *Silver Nanoparticle Transparency Film*, Mitsubishi Imaging (MPM), Inc., Available online at http://diamond-jet.com/silvernanoparticleink-1-1-1-1.aspx.

[29] "Test Method for Determining the Electrical Resistivity of a Printed Conductive Material", Designation: F 1896-98 (Reapproved 2004).

[30] A. Hernandez, E. Martin, J. Margineda, and J. M. Zamarro, "Resonant cavities for measuring the surface resistance of metals at X-band frequencies," *J. Phys. E: Sci. Instrum*., vol. 19, pp. 222–225, 1986.

[31] F. Costa, "Surface Impedance Measurement of Resistive Coatings at Microwave Frequencies" *IEEE Transaction on Instrumentation and Measurement*, vol. 62, no. 2, pp. 432-437, February 2013.

[32] S. Manzari, G. Marrocco, "Modeling and Applications of a Chemical-Loaded UHF RFID Sensing Antenna with Tuning Capability", *IEEE Trans. Antennas and Propagat*. Vol. 62, N.1, pp 94-101, Jan. 2014

[33] M. Shahpari and D. V. Thiel, "The Impact of Reduced Conductivity on the Performance of Wire Antennas," in I*EEE Transactions on Antennas and Propagation*, vol. 63, no. 11, pp. 4686-4692, Nov. 2015.

[34] G. Marrocco, "Gain-optimized self-resonant meander line antennas for RFID applications", IEEE Antennas and Wireless Propagation Letters, vol.2, pp.302-305, 2003.

[35] Matsuda, Yu, et al. "Electric Conductive Pattern Element Fabricated Using Commercial Inkjet Printer for Paper-Based Analytical Devices.", *Analytical Chemistry*, Vol. 87, no. 11, pp 5762-5765, May 2015.

[36] G. Saggio, et al. "Resistive flex sensors: a survey", *Smart Materials and Structures*, vol. 25, no.1, December 2015.

[37] S. Amendola, C. Occhiuzzi, A. Ajovalasit, M.A. Sabatino, C. Dispenza, G. Marrocco, (2015, September). "Dielectric characterization of biocompatible hydrogels for application to epidermal RFID devices, *IEEE Microwave Conference (EuMC), 2015* pp. 379-382, 2015.

[38] S. Amendola and G. Marrocco, "Optimal Performance of Epidermal Antennas for UHF Radiofrequency Identification and Sensing", in *IEEE Transactions on Antennas and Propagation,* Nov. 2016.

[39] Najafabadi, Alireza Hassani, et al. "Biodegradable nanofibrous polymeric substrates for generating elastic and flexible electronics, Advanced Materials, vol. 26, no.33. pp. 5823-5830, 2014.